Characterization of Maraging Steel Fabricated with Metal Laser Sintering Hybrid Milling

Emmanuel U. Enemuoh, Jose Carrillo, Joseph Klein, Austin Cash, Drew Bergstrom
Mechanical & Industrial Engineering, University of Minnesota Duluth
1305 Ordean Court, 105 VKH, Duluth, MN 55812

Abstract

Direct Metal Laser Sintering (DMLS) additive manufacturing is increasingly being used in industrial applications such as mold and tool manufacturing due to its capabilities in building free form complex shapes that are otherwise challenging to manufacture by conventional methods. Researchers are still making effort to build knowledge database and understanding of the mechanical behavior of components made with additive manufacturing. Matsuura USA has developed a DMLS Hybrid Milling (DMLS-HM) to improve the quality of parts made with conventional DMLS process and a senior design capstone team at University of Minnesota Duluth (UMD) has been tasked to design experiments to test and characterize Maraging steel 300 (MS 300) parts built with Matsuura LUMEX machine. ASTM-compliant tensile, hardness and density tests were performed following ASTM standard E8.

The average results from the 28 tension tests resulted in a yield strength of 1111 MPa (161.2 ksi), ultimate tensile strength (UTS) of 1205 MPa (174.8 ksi), and a modulus of elasticity of 153.7 GPa (22,300 ksi). The strain at yield was 0.009, 0.022 at UTS, and 0.14 at fracture. Hardness tests were performed on 10 samples in compliance with ASTM standard E18. All faces of each specimen were tested, and results were reported in the Rockwell 'C' scale. Hardness tests resulted in an average hardness value of 36.0 HRC. Density measurement was conducted on 10 samples following ASTM standard B962 and B311. These tests resulted in an average density of 8.184g/cm^3. To further analyze the fracture plane of tensile test specimen, a scanning electron microscope (SEM) was used to examine the surfaces and percent composition analysis was performed. The percent weight composition was consistent with the alloy composition from the metal powder supplier.

The results from the study will enhance learning of DMLS-HM process and will provide better understanding of the process capabilities and mechanical properties of the MS 300 produced by DMLS-HM for mold industry application.

Keywords: Capstone, Undergraduate Design, Additive Manufacturing, Undergraduate Research

1. Introduction

Additive Manufacturing (AM) is defined by ASTM as the "process of joining materials to make objects from 3D model data usually layer upon layer, as opposed to subtractive manufacturing technologies such as traditional machining" (ASTM 2012). Initially, the mission of this innovative technology was to build prototypes quickly for modeling and testing purposes, but the technology advanced quickly, and applications have widened into mold industry, medical, sculpture, architecture, manufacturing industrial and many other domains. Some advantages of AM over other manufacturing techniques include: geometrical flexibility, no tool and fixture requirement, efficient use of energy, reduced time and cost (Manfredi et al. 2014, Cabrini et al. 2016, Lindemann and Jahnke 2017). Amongst the AM processes, powder bed fusion processes such as DMLS or EBM draw more attention due to their ability to make functional parts (Wang et al. 2002, Rossi et al. 2004, and Sing et al. 2006). DMLS AM process uses powerful laser energy source to scan and melt a continuous line of powder, one layer at a time. A complex 3-D part can be fabricated by sequential layer creation on top of each other. (Kruth et al. 2005). The process parameters: scan speed, layer thickness, powder thickness, hatch size, scan path pattern and laser power will affect the outcome of DMLS process. A part's mechanical properties, surface roughness and geometrical accuracy can all be affected by the settings of these control factors. Over the years, several researchers have reported the effects of these DMLS process parameters on the quality of the part fabricated. Pogson et al. (2003) reported that higher scan speeds lead to thinner and longer molten pool while at lower scan speeds more material stay in the molten state. Conventional DMLS parts are fabricated with high surface roughness and density with smaller distance between laser scans as observed by Zhu et al. (2005). It was reported that among the DMLS process parameters, laser scanning speed and laser power have most significant effect on the density of the fabricated parts Wang et al. (2016).

To improve quality characteristics of fabricated parts and the economy of the process, DMLS hybrid milling (DMLS-HM) was introduced. In DMLS-HM process, an end mill with very high spindle speed and high feeding rate is incorporated with the laser sintering to attain high-precision machining. The sintering and milling of the part is repeated to build from bottom to top layers of a complex part shape. Compared to conventional DMLS, there is limited study on the evaluation of mechanical properties of parts fabricated with DMSL-HM process. This research project is aimed at characterizing non-aged Maraging steel 300 (MS 300) parts fabricated with DMLS-HM process.

2. Maraging Steel 300

Maraging is classified as a low-carbon, ultra-high strength steel. Its name is derived from a portmanteau of 'martensite' – a very high strength phase of steel – and 'aging.' Maraging Steel 300 can be age-hardened to increase its strength and hardness properties, but this project is limited to characterization of components as-built with LUMEX machine. The alloy is supplied in a gas atomized powder form with composition by mass given in Table 1.

Table 1 Maraging Steel 300 Powder, Percent Composition by Mass

Content	Nickel	Cobalt	Molybdenum	Titanium	Silicon	Manganese	Phosphorus	Sulfur	Iron
%	17- 9	7 -10	4.5 – 5.2	0.3-1.2	≤.10	≤.15	≤.03	≤.01	Bal.

3. Experimental Procedure

3.1. Direct Metal Laser Sintering Hybrid Milling Process

Matsuura LUMEX was used in manufacturing the test samples. LUMEX is a single machine platform integrating a fiber laser for state of the art metal sintering in a 256mm by 256mm by 300mm space and a machining center for performing high accuracy, high speed milling. All specimens were printed vertically, in the positive z-direction as shown in Figure 1. The process comprises of three main phases: squeezing, laser sintering and milling. Squeezing is performed by laminating metal powder to a thickness of 0.05 mm on the base plate located on the table as illustrated in Figure 2(a). Then a 400 Watts high efficient Yd fiber laser of high beam quality is used to sinter the metal powder into the desired product shape bonded to the processing table. The upper surface of the table is heated to alleviate rapid temperature changes resulting from laser sintering, therefore, increasing the sintering precision. After the metal powder is sintered, the LUMEX squeezes and supplies metal powder with a thickness of 0.05 mm to form the next layer and sinter all the laminated layers. Squeezing and laser sintering steps are repeated 10 times until thickness of 0.5 mm (0.019 in) is achieved, then, the LUMEX goes to the phase of milling as illustrated with Figure 2(b). An end mill incorporating oil-air lubricated spindle with spindle speed of 45000 rpm and a 1/10 taper special BT20 tool shank performs milling of the contour of the part precisely to a finish. High-speed feeding (X/Y: 60 m/min (2.36 ipm) and 30 m/min (1.18 ipm)) are used to attain high-precision machining. The LUMEX repeats the sintering and milling of the part to build from the bottom layer to top layers, irrespective of the complexity of the internal shape.

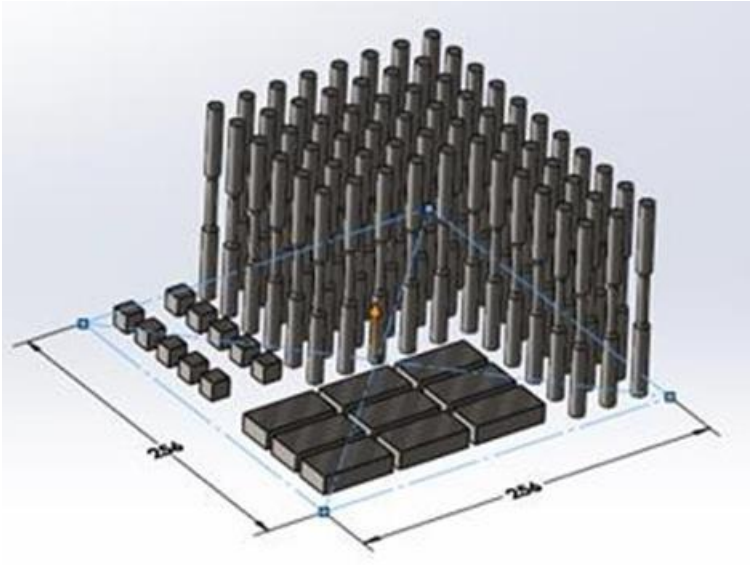

Figure 1 Build Layout for Samples. Yellow Arrow indicates Print Direction.

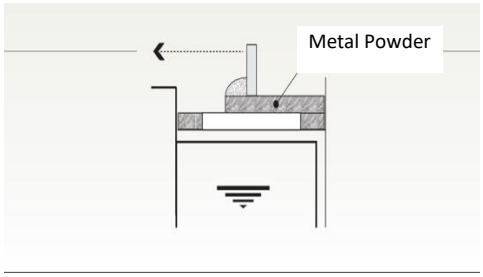

Figure 2(a) Squeezing of metal powder

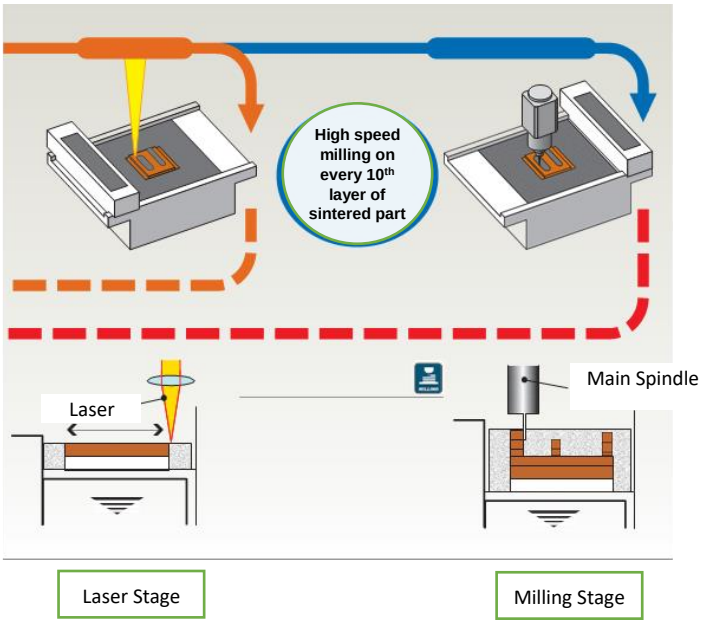

Figure 2(b) Metal laser sintering and milling phases (Matsuura, 2017)

3.2 Samples Preparation

The specimens for the material testing were designed in accordance with the applicable ASTM standards to ensure comparative analysis of test results. The specimen for the tensile tests (Figure 3) is designed to the standard geometry listed in ASTM Standard E8. The critical geometry of this specimen is the necked down region that ensures the specimen breaks in a predictable manner.

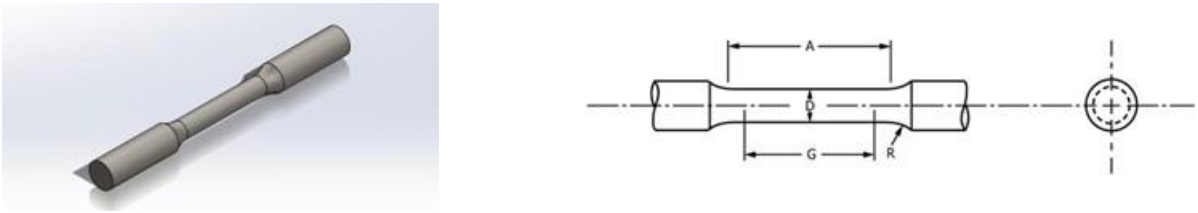

Figure 3 Tensile Test Specimen (ASTM E8)

Table 2 ASTM standard dimension for tensile specimens

Feature	Dimension
G - Gauge Length	1.000 ± 0.005 in
D - Diameter	0.250 ± 0.005 in
R - Radius of Fillet (min)	3/16 in
A - Length of Reduced Section (min)	1.25 in
Ends*	Diameter = 0.375 in, Length = 1.043 in

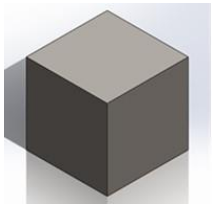

Figure 4a. CAD Model of Density Specimen

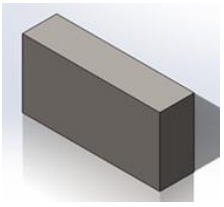

Figure 4b. CAD Model of Hardness Specimen

Table 3 Dimension of specimens for hardness and density

	Hardness	Density
Length (inches)	2.0	0.5
Width (inches)	1.0	0.5
Thickness (inches)	0.5	0.5

The hardness specimens shown in Figure 4a were designed in compliance with ASTM Standard E18. The standard requires the thickness of the specimen to be ten times the indenter depth. This requirement is to ensure that no deformation occurs on the bottom surface of the specimen, therefore, skewing the results. Hardness test was conducted on all faces at least four times, then the average of these tests was taken. Measurement results greater than ±3σ were considered invalid results and removed from analysis.

4. Result and Discussion

4.1. Mechanical Properties - Tension

Tension tests were performed on 28 samples of MS 300 using MTS Landmark tensile testing machine with 55 Kips load cell. All tests were conducted following the ASTM Standard E8. The stress strain data were used to evaluate the mechanical properties: yield strength (**σ_Y**), ultimate tensile strength (**σ_{UT}**), modulus of elasticity (**E**), and ultimate tensile strain (**ε_{UT}**). Table 5 shows the average mechanical properties and standard deviation measurements of the samples of MS 300 tested. Figure 5 shows the stress strain curves of the MS 300 samples and illustrates that the 28 samples show minimal variation between each other.

Table 5 Maraging Steel Tensile Properties

	SI		***Imperial***	
	Mean	**Standard deviation (±1σ)**	**Mean**	**Standard deviation (±1σ)**
σ_{UT}	1205.5 MPa	14 MPa	174,846 psi	2031 psi
σ_Y	1111.5 MPa	14 MPa	161,214 psi	2031 psi
ε_{UT}	0.0223	0.003	0.0223	0.003
ε_Y	0.0093	0.0002	0.0093	0.0002
E	153.7 GPa	1.3 GPa	22,291 ksi	189 ksi

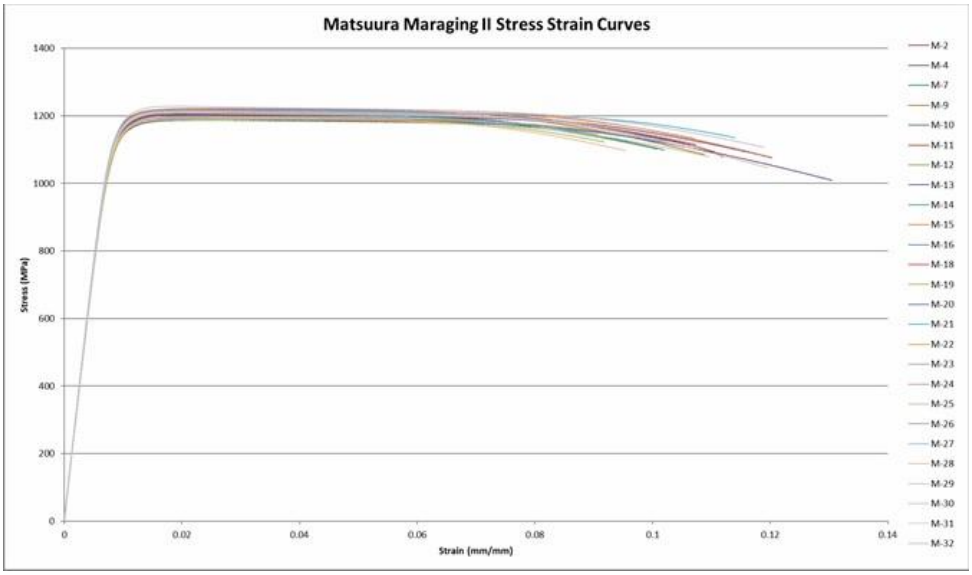

Figure 5: Stress-Strain Curves of the MS 300 Samples from Tension Tests*

*Note: Extensometer removed before fracture. These curves do not show stress/strain at fracture.

4.2. Maraging Steel 300 Properties Compared to S7 Tool Steel and Titanium (Ti-6Al-4v)

ASTM standard E8 was used to conduct tension tests on S7 tool steel using the MTS material testing equipment like tests conducted on the MS 300. The mechanical properties evaluated are summarized in Table 6. Figure 6 shows the plot of their mechanical properties showing that the ultimate tensile property of non-age hardened MS 300 is superior to S7 Tool steel and Titanium alloy by 37% and 21% respectively. The measurements of their yield strength show that Maraging steel is stronger than S7 Tool steel and Titanium alloy by 42% and 21% respectively. The S7 shows 5% higher stiffness property than MS 300 while MS 300 shows 26% higher stiffness property than Titanium. These properties show that MS 300 made with DMLS-HM has capabilities to serve as mold material.

Table 6 Summary of Mechanical Properties of MS 300, S7 steel, and Ti-6Al-4v

	MS 300	S7 Tool steel	Titanium (Ti-6Al-4v)
σ_{UT} MPa (psi)	1205.5 (174,846)	761(110,374)	950 (138000)
σ_{Y} MPa (psi)	1111.5 (161,214)	644 (93,404)	880 (128,000)
E GPa (psi)	153.7 (22,291)	162.7 (23,598)	113.8 (16,500)

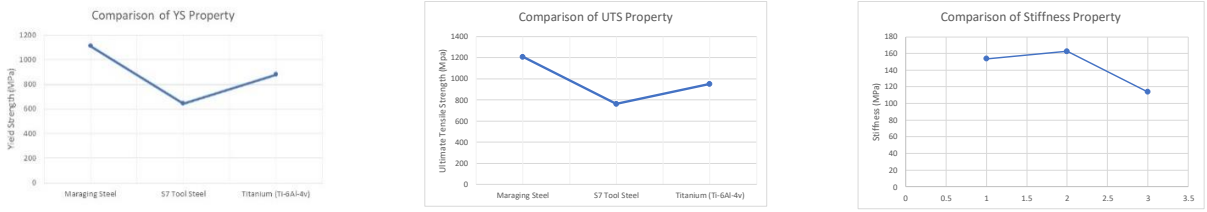

Figure 6 Comparison of Tension Mechanical Properties

4.3 Mechanical Properties – Hardness

Hardness test was conducted using Fowler Rockwell hardness tester and following ASTM E18 standard. This machine was verified to be accurate and precise from a standard Rockwell hardness coupon that was tested preceding the MS 300 samples. Dwell time used for the hardness testers was four seconds, and results less than 24 HRC or above 48 HRC were considered invalid test results. The average hardness was 36 HRC. This is comparable to the hardness of annealed Titanium Ti-6Al-4V (Grade 5).

4.4. Physical Property - Density

In compliance with ASTM standard B311-17, the density of ½" cubes were determined using an analytical balance as shown in Figure 7. The standard of procedure was chosen because the parts sintered from LUMEX machine have less than two percent surface porosity.

The construction of a stage and a specimen holder was required to use Archimedes' Principle. Wire diameter was chosen as 0.12 mm in accordance to the standard for specimens with mass less than 50g to minimize its effect on the results. The analytical balance was set to the thousandths place and mass measurements of specimens in air and water were taken. Density was calculated using the Equation 1, utilizing a known force buoyant. The temperature of the water was 20°C which was used to find E in the Equation 1. Taking the density of water to be 0.9982 g/cm^3 at 20°C, the average density of all the components was 8.208g/cm^3, with a range of ±0.044g/cm^3. Although MS 300 has higher values than both S7 and Ti-6Al-4V, it should be noted that Ti-6Al-4V has a density of 4.43g/cm^3, which is roughly half the density of MS 300.

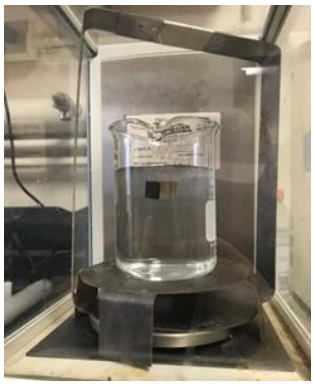

Figure 7: Testing Apparatus inside Analytical Balance used for Density Determination

$$D = \frac{A}{[A-(B-C)]/E} \qquad (1)$$

Where:
D = density of test specimen, g/cm^3
A = mass of test specimen in air, g
B = apparent mass of test specimen and specimen support in water, g
C = mass of specimen support immersed in water, g.
F = mass of test specimen in water with mass of specimen supported tared, g, and
E = density of water in g/cm^3.

4.5 Microstructure Analysis of Percent Composition

A Scanning Electron Micrograph (SEM) was used to determine average percent composition of the alloy on the fractured surfaces of the tensile specimens. The broken specimens from tension tests had two distinct fracture characteristics. They appeared roughly half failed by shear, and the other half exhibited 'cup and cone' fracture. The main way that these specimens were differentiated was by the angle between the normal vector of the fracture plane and the x-axis (or ground). For the shear fracture surfaces, the angle was roughly 45 degrees, while cup and cone fracture surfaces were roughly 0 degree. The specimen used for the percent composition analysis was the 'cup' portion. On Figure 9, spectrum 1 represents ductile region of fracture, while spectrum 2 represents the brittle region. Table 7 shows the result of the percent composition analysis. These results from the SEM are only rough estimates (as the surface was not cleaned or polished) but are very close to the expected results from the MS 300 powder composition showing that the distribution of alloy is not changed by the DMLS-HM process.

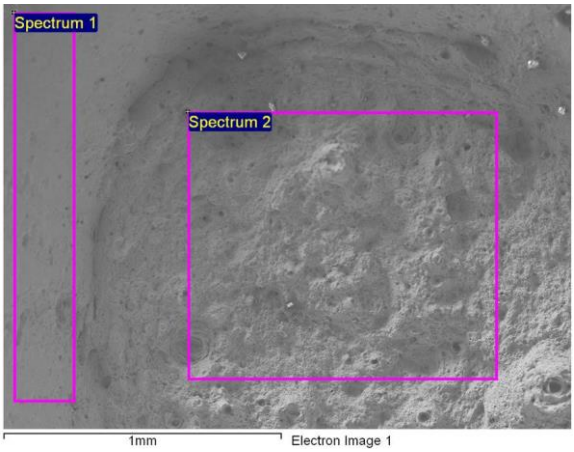

Figure 9 Percent Composition Analysis with Scanning Electron Micrograph

Table 7 Percent Composition (Weight %) Analysis Using SEM

Spectrum	In stats.	Cl	Ti	Fe	Co	Ni	Mo	Total
Spectrum 1	Yes	0.24	0.66	70.81	9.63	15.46	3.21	100.00
Spectrum 2	Yes		0.70	70.11	9.49	15.49	4.22	100.00

5 Conclusion

Comprehensive test and analysis of MS 300 mechanical properties fabricated with LUMEX direct metal laser sintering hybrid milling have been conducted and the following results were obtained:

- The average mechanical properties from 28 samples of tension tests resulted in average yield strength of 1111 MPa (161.2 ksi), ultimate tensile strength (UTS) of 1205 MPa (174.8 ksi), and a modulus of elasticity of 153.7 GPa (22,300 ksi). The strain at yield was 0.009, 0.022 at UTS, and 0.14 at fracture.
- It was found that the ultimate strength property of DMLS-HM Maraging steel 300 at non-age hardened state is superior to S7 Tool steel and Titanium alloy by 37% and 21% respectively. The measurements of their yield strength showed that Maraging steel 300 is stronger than S7 Tool steel and Titanium alloy by 42% and 21% respectively. The S7 shows 5% higher stiffness property than MS 300 while MS 300 shows 26% higher stiffness property than Titanium.
- Hardness test was performed on all surfaces of DMLS-HM MS 300 specimen in compliance with ASTM standard E18 and results were reported with an average hardness value of 36.0 HRC.
- Density test was conducted on DMLS-HM MS 300 samples in compliance with ASTM standard B962 and B311 and result was reported with an average density of 8.184g/cm^3.
- A scanning electron microscope (SEM) was used to observe and analyze the fracture surfaces of the DMLS-HM tensile specimens and their percent composition. The percent composition on the fracture surface is consistent with the composition specified by the manufacturer of the MS 300 powder.

Acknowledgement

This research and senior design project was funded by Matsuura USA and is highly appreciated.

References

ASTM Standard F2792-12a, 2012, "Standard Terminology for Additive Manufacturing Technologies", ASTM International, West Conshohocken, PA, 2012, DOI: 10.1520/F2792-10, www.astm.org.

ASTM Standard A370, 2017, “Standard Test Methods and Definitions for Mechanical Testing of Steel Products,” ASTM International, West Conshohocken, PA, 1953, DOI: 10.1520/A0370-17A, www.astm.org.

ASTM Standard B311, 2017, “Standard Test Methods for Density of Powder Metallurgy (PM)Materials Containing Less Than Two Percent Porosity,” ASTM International, West Conshohocken, PA, 2008, DOI: 10.1520/B0311-17, www.astm.org.

ASTM Standard B962, 2017, “Standard Test Methods for Density of Compacted or Sintered Powder Metallurgy (PM) Products Using Archimedes’ Principle,” ASTM International, West Conshohocken, PA, 2008, DOI: 10.1520/B0962-17, www.astm.org.

ASTM Standard E8, 2016, “Standard Test Methods for Tension Testing of Metallic Materials,” ASTM International, West Conshohocken, PA, 1924, DOI: 10.1520/E0008_E0008M-16A, www.astm.org.
ASTM Standard E18, 2017, “Standard Test Methods for Rockwell Hardness of Metallic Materials,” ASTM International, West Conshohocken, PA, 1932, DOI: 10.1520/E0018-17E01, www.astm.org.
ASTM Standard E986, 2017, “Standard Practice for Scanning Electron Microscope Beam Size Characterization,” ASTM International, West Conshohocken, PA, 1955, DOI: 10.1520/E0986-04, www.astm.org.
Cabrini, M., et al., 2016. Evaluation of corrosion resistance of Al–10Si–Mg alloy obtained by means of Direct Metal Laser Sintering. Journal of Materials Processing Technology, 231, 326– 335.
Kruth, J.-P., et al., 2005. Binding mechanisms in selective laser sintering and selective laser melting. Rapid Prototyping Journal, 11 (1), 26–36.
Lindemann, C.F.W., and Jahnke, U., 2017. 11 – Modelling of laser additive manufactured product lifecycle costs A2 – Brandt, Milan. Laser Additive Manufacturing. Woodhead Publishing, Vol 1, 281–316. Available from: http://dx.doi.org/10.1016/B978-0-08-100433-3.00011-7.
Manfredi, D., et al., 2014. Direct Metal Laser Sintering: an additive manufacturing technology ready to produce lightweight structural parts for robotic applications. La metallurgia italiana, 1 (10), 15–24.
Matsuura. (2017). LUMEX Hybrid Metal 3D Printer [Brochure]. Fukui City, Japan: Author.
Pogson, S.R., et al., 2003. The production of copper parts using DMLR. Rapid Prototyping Journal, 9 (5), 334–343.
Renishaw. (2017). Maraging Steel M300 powder for additive manufacturing [Brochure]. New Mills, Kingswood, Wotton-under-Edge, Gloucestershire, England: Author.
Rossi, S., Deflorian, F., and Venturini, F., 2004. Improvement of surface finishing and corrosion resistance of prototypes produced by direct metal laser sintering. Journal of Materials Processing Technology, 148 (3), 301–309.
Sing, S.L., et al., 2016. Laser and electron-beam powder-bed additive manufacturing of metallic implants: A review on processes, materials and designs. Journal of Orthopedic Research, 34 (3), 369–385.
Titanium Ti-6Al-4V (Grade 5), Annealed. (2017). Retrieved April 12, 2018, from http://asm.matweb.com/search/SpecificMaterial.asp?bassnum=mtp641
Wang, X., et al., 2002. Direct selective laser sintering of hard metal powders: experimental study and simulation. The International Journal of Advanced Manufacturing Technology, 19 (5), 351–357.
Wang, X., et al., 2016. Densification of W–Ni–Fe powders using laser sintering. International Journal of Refractory Metals and Hard Materials, 56, 145–150.
Zhu, H.H., Fuh, J. Y. H., and Lu, L., 2005. Microstructural evolution in direct laser sintering of Cu-based metal powder. Rapid Prototyping Journal, 11 (2), 74–81.

Biographical Information

Emmanuel Enemuoh is an Associate Professor of Mechanical & Industrial Engineering at University of Minnesota Duluth (UMD). He earned his Ph.D. and M.Sc. degrees in Mechanical Engineering, 2000 and 1996 respectively from the University of Missouri Columbia. He was a Post-Doctoral Fellow at Intelligent Systems Center at University of Missouri Rolla, researching "Aged Aircraft Issues-Nondestructive Evaluation, Repairs of metallic and composite materials." Dr. Enemuoh teaches in the areas of material science, material processing, nondestructive evaluation techniques, multidisciplinary senior design, and global sustainability.

Jose Carrillo is an Adjunct Professor with Mechanical & Industrial Engineering Department at UMD. He received his M.S. degree in Manufacturing Engineering from University of Southern California, Los Angeles,1993. He has worked as Senior Manufacturing Engineer at various companies and worked as Senior Operations Engineer at Northrop Grumman, United Defense, and BAE Systems. He also served as Program Manager at Cirrus Design Corp. and Alion Science and Technology. His teaching interests include: Intro to Solid Modeling, Intro to Engineering, CADCAM, multidisciplinary senior design, machine design and engineering professionalism.

Joe Klein graduated from the University of Minnesota Duluth in May of 2018 with a degree in Mechanical Engineering. His experiences as a project engineering intern at Polaris Industries have taught the importance of attention to detail and proper project planning. The fast-paced environment exposed him to many different aspects of engineering during his 5-month internship including research & development, testing, manufacturing, quality control, and design.

Drew Bergstrom is a senior studying mechanical engineering at the University of Minnesota Duluth graduating in Spring of 2018. During his internship at Saginaw he built and re-designed multiple electro-mechanical assemblies to specification for pipeline, shipping and government applications. He is a registered associate in SolidWorks, and is proficient in all Microsoft office products, MATLAB, Fluent, and Ansys software models.

Austin Cash graduated with degree in Mechanical Engineering from the University of Minnesota Duluth. This past summer, he gained valuable experience in manufacturing and product development through his internship with Malco Products SBC. The work he performed consisted of the complete design of a new hand tool. His involvement with this project included SolidWorks modeling of the tool, fixture design, progressive die design, and the implementation of new manufacturing processes.